

General Disclaimer

One or more of the Following Statements may affect this Document

- This document has been reproduced from the best copy furnished by the organizational source. It is being released in the interest of making available as much information as possible.
- This document may contain data, which exceeds the sheet parameters. It was furnished in this condition by the organizational source and is the best copy available.
- This document may contain tone-on-tone or color graphs, charts and/or pictures, which have been reproduced in black and white.
- This document is paginated as submitted by the original source.
- Portions of this document are not fully legible due to the historical nature of some of the material. However, it is the best reproduction available from the original submission.

"Made available under the
in the interest of early and rapid
semination of Earth Resources Survey
Program information and without liability
for any use made thereof."

E84-10045

CR-174612



FOURTH QUARTERLY REPORT

ON

**"SPECTRORADIOMETRIC CALIBRATION OF THE
THEMATIC MAPPER AND MULTISPECTRAL SCANNER SYSTEM"**

Contract Number NAS5-27382
For the Period: 1 August 1983 - 1 November 1983

NASA/Goddard Space Flight Center

Greenbelt, MD 20771

James M. Palmer, Co-Investigator
Philip N. Slater, Principal Investigator

Optical Sciences Center
University of Arizona
Tucson, Arizona 85721



(E84-10045) SPECTRORADIOMETRIC CALIBRATION
OF THE THEMATIC MAPPER AND MULTISPECTRAL
SCANNER SYSTEM Quarterly Report, 1 Aug. - 1
NOV. 1983 (Arizona Univ., Tucson.) 16 p
HC A02/MF A01 CSCL 08B

INTRODUCTION

This is the fourth quarterly report on Contract NAS5-27382 entitled, "Spectroradiometric Calibration of the Thematic Mapper and the Multispectral Scanner System." In this report, we describe the design of the spectroradiometer now under construction for atmospheric and surface measurements at White Sands.

DESIGN OF THE SPECTROPOLARIMETER

Statement of problem

The spectropolarimeter is to be used to make measurements of incident radiation to characterize the atmospheric extinction as a function of wavelength. As mentioned in previous reports, the optical depth ($\tau'_{ext}(\lambda)$) can be found using the Langley plot method, and the ground reflectance ($\rho(\lambda)$) can be determined by comparing barium sulfate radiance measurements with ground radiance measurements. These two quantities, $\tau'_{ext}(\lambda)$ and $\rho(\lambda)$, are then input into our radiative transfer program to estimate the absolute radiance at the satellite. As a further check on the accuracy of the transfer program, the sky radiance can be measured and compared to that predicted by the program. Shaw et al.¹ demonstrated the Langley plot method in their observations of the solar irradiance at a number of wavelengths.

The following functions define the scope of the instrument's observation capability:

- 1) To measure the solar irradiance at a number of wavelengths as a function of air mass for Langley plot analysis in order to generate the optical depth $\tau'_{ext}(\lambda)$.
- 2) To measure the ground radiance to determine the absolute ground reflectance $\rho(\lambda)$.
- 3) To measure the sky radiance as a method of checking the accuracy of our radiative transfer program.

Initial considerations

The design of the spectropolarimeter was based on calculations of the spectral power distribution of the sun, the sky, and the ground, under a variety of conditions. Table I shows the maximum and minimum spectral irradiances expected at a number of wavelengths at the entrance pupil of the optical system. The minimum radiance level anticipated was estimated to be $0.044 \text{ mW/cm}^2\text{sr}$ at the entrance pupil due to the reflectance of damp soil (0.1) and a solar zenith angle of 75 degrees. The maximum level was assumed to be due to exo-atmospheric solar irradiance. The bandwidths were chosen following Shaw.²

Table I

λ (μm)	$\Delta\lambda$ (nm)	E_λ (mW/cm ² · μm)	$E \cdot \Delta\lambda$ (mW/cm)	L_λ (mW/cm ² ·sr· μm)	$L \cdot \Delta\lambda$ (mW/cm ² ·sr)
0.40	10.0	207.2	2.07	4.43	0.044
0.44	10.0	224.4	2.24	7.93	0.079
0.53	10.0	226.5	2.27	8.44	0.084
0.60	10.0	204.5	2.05	7.87	0.079
0.66	10.0	187.7	1.88	7.35	0.074
0.78	10.0	152.6	1.53	6.16	0.062
0.86	20.0	121.2	2.42	5.00	0.100
1.04	40.0	85.0	3.40	3.55	0.142

where: λ is the wavelength

$\Delta\lambda$ is the spectral bandwidth for each wavelength

E_λ is the solar spectral irradiance at the entrance pupil

$E \cdot \Delta\lambda$ is the solar irradiance at the entrance pupil times bandwidth

L_λ is the minimum expected spectral radiance at the entrance pupil

$L \cdot \Delta\lambda$ is the minimum radiance at the entrance pupil times bandwidth

To adequately cover the spectral range indicated in Table I, it was felt that a silicon photodiode operated in the unbiased mode was the best choice because of its:

- 1) Small size and durability (photomultiplier tubes are large and fragile).
- 2) Adequate spectral coverage for the range 400 nm to 1100 nm.
- 3) Linear performance over a large (7 decade) range.
- 4) Well understood operation.

The detector chosen was the UV444-B supplied by the EG&G Corporation.³ This detector has also been used in our lab as part of an ongoing study of self-calibrated diodes and so is familiar to us.

Table II shows the approximate responsivity of this detector as well as I_{\max} and I_{\min} , the maximal and minimal currents outputted by the detector. Note that both of these are dependent upon the entrance pupil area and also that I_{\min} depends on solid angle. We chose a 15° full field for our instrument because we have found that a 15° full field is sufficient to average out local surface irregularities when looking at the ground from a height of 2 meters (as will be done with this instrument). Table III shows I_{\min} for three different apertures (0.01cm², 0.1cm², and 1.0cm²). If we assume a minimal current requirement of 1 nanoamp, we see that all three satisfy this.

It was also decided early on to do our gain compensation optically by using neutral density filters. Table IV shows I_{\max} divided by 10,000 (ND 4.0) as a function of three apertures (0.1cm², 1.0cm², and 10.0cm²). Based on these values we chose an entrance aperture of 2 cm diameter. This value was chosen because it corresponded well with typical manufacturer stock optical components.

Table II

λ (μm)	$R(\lambda)$	I_{\max} ($\mu\text{a}/\text{cm}^2$)	I_{\min} ($\mu\text{a}/\text{cm}^2 \cdot \text{sr}$)
0.40	0.200	0.414	8.8
0.44	0.250	0.560	19.8
0.53	0.350	0.795	29.4
0.60	0.400	0.820	31.6
0.66	0.480	0.902	35.5
0.78	0.620	0.949	38.4
0.86	0.650	1.573	65.0
1.04	0.200	0.680	28.4

where: $R(\lambda)$ is the detector responsivity

Table III

λ	I_{\min} (μa)		
	0.01 cm^2	0.1 cm^2	1 cm^2
0.40	4.73	47.3	473
0.44	10.64	106.4	1064
0.53	15.80	158.0	1580
0.60	16.99	169.9	1699
0.66	19.08	190.8	1908
0.78	20.64	206.4	2064
0.86	34.94	349.4	3494
1.04	15.27	152.7	1527

Table IV

λ	I_{\max} (μa)		
	0.1 cm^2	1 cm^2	10 cm^2
0.40	4.14	41.4	414
0.44	5.60	56.0	560
0.53	7.95	79.5	795
0.60	8.20	82.0	820
0.66	9.02	90.2	902
0.78	9.49	94.9	949
0.86	15.73	157.3	1573
1.04	6.80	68.0	680

A full field angle of 5° was chosen for observations of the sky under the minimal lighting conditions corresponding to a 75 degrees solar zenith angle. Such a field angle will not induce a significant averaging error while providing a solid angle sufficient to give a high SNR under minimum lighting conditions. The predicted currents for this configuration are very similar to those found above in Tables III and IV.

Choice of optical components

For solar observations as input to Langley plot routines, a fairly broad spectral coverage is needed to characterize aerosol and gaseous optical depths. 10 wavelengths were chosen between 0.4 μm and 1.04 μm and they are 0.400, 0.420, 0.440, 0.525, 0.600, 0.660, 0.780, 0.860, 0.940, 1.040 μm . Six are in regions of little or no gaseous absorption (0.400, 0.420, 0.440, 0.780, 0.860, 1.040 μm), three are in the Chappuis band of ozone absorption (0.525, 0.600, 0.660 μm), and one is in the water vapor absorption band at 0.94 μm . A nominal bandpass of 10 nm was chosen for the filters with the exception of 20 nm at 0.940 μm and 40 nm at 1.040 μm .

The same spectral filters were chosen for sky observations. It was decided that direct solar flux should be attenuated through the use of neutral density filters so that the irradiance levels at the detector would be about the same as that due to diffuse flux from the sky. Polarization measurements are to be made as a means of correcting radiance calculations since it has been suggested that errors of several percent could be encountered if polarization were not accounted for.

Checks of some of the neutral polarization points (Babinet, Arago, etc.) will also prove helpful in comparing the radiative transfer calculations with real data. Polarization measurements require a polarizer and a retardation plate. The ideal plate should be quarter wave but this would require 10 separate plates. However, it can be shown* that if one knows the retardation that the plate provides, then only four measurements are required for the Stoke's parameters. The difference between the ideal $\lambda/4$ and, for example, a $\lambda/40$ plate is that the equations for the $\lambda/4$ case are much simpler than the $\lambda/40$ case. The measurements are also more sensitive to polarization variations when the $\lambda/4$ plate is used. The four measurements that are required are: two at 90 degrees to each other with or without the waveplate, and two directly between these two, one with and one without the waveplate. The sum of the first two measurements gives the total radiance or irradiance while the second two are needed to determine the state and orientation of the polarized beam.

The basic instrument design utilizing the above components is shown in Fig. 1a. Light first passes through a window which protects the internal elements from atmospheric contamination. Next, the neutral density and spectral filters are located in the collimated portion of the beam. In particular, note that the maximum departure from normal incidence for the spectral filters is 2.5 degrees. This produces an insignificant shift and change in the filter shape and position. The imaging lens immediately following the spectral filter creates a converging beam. Most radiometer designs employ a field stop at the focal point of this lens followed by a relay lens, but space

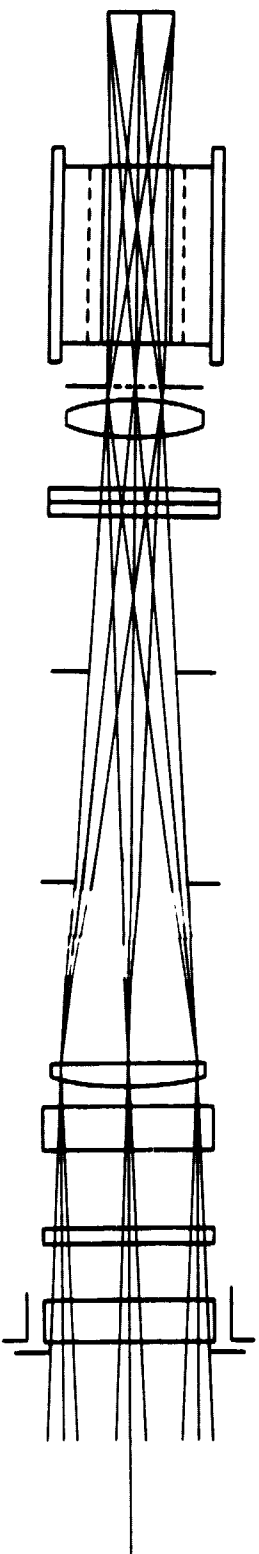


Fig. 1a. Sun and sky optical configuration.

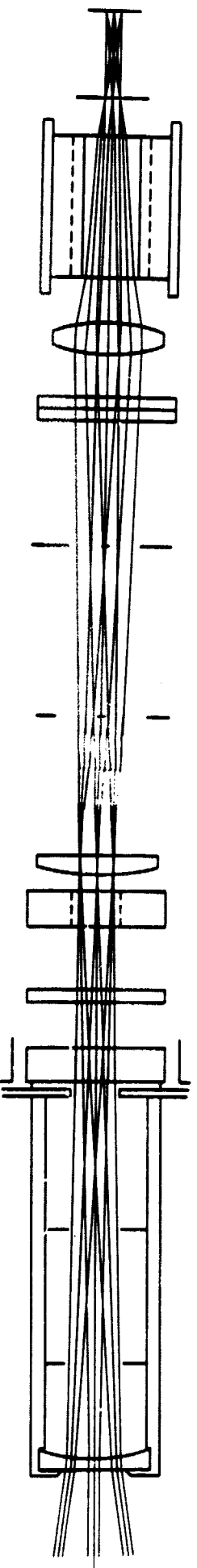


Fig. 1b. Ground looking optical configuration.

considerations prevented this. Here the relay lens comes before the focal plane of the imaging lens and the field stop. The relay lens images the entrance pupil onto the detector, providing uniform illumination over the detector with no light loss (which would occur if a diffusing plate were to be used). To achieve a 5 degree unvignetted full field required that the detector be 1 cm diameter. A Glan-Thompson prism polarizer was chosen as the best polarizer for our purposes because of its large spectral range, viewing angle of 15 degrees, and its extinction ratio of 1.0E-05. By locating the polarizer behind the field stop, a 1 cm clear aperture polarizer can be used. This represents a large monetary savings over the next larger size (1.2 cm, 50% more expensive). The wave plate retarder has to be positioned in front of the polarizer and the only available space was between the two lenses. The wave plate was chosen to be quarter wave at 500 nm because at this wavelength it is not half wave for any of the filters. The variance in retardation of the filters chosen is $\lambda/3.2$ to $\lambda/8.32$ from 400 to 1040 nm respectively. Two detectors are to be used, the first a standard silicon photodiode. It will respond in the range 0.4 to 1.2 μm and so will be used with the 10 filters discussed above. The wavelength range out to 2.4 μm will be studied using a different detector and different filters. Provisions are being made to allow the inclusion of more filters and another detector in the design although they have not been defined as yet. In this way we can proceed with the current design and update it at a later time.

For use as a ground looking instrument, a full field of 15° was chosen to smooth out ground radiance variations when the instrument is

located 2 meters above the ground. We did not want to change the basic instrument design and so a negative lens is located in front to convert the 15 degree field into a 5 degree field entering the instrument. A new field stop is located behind the polarizer. When the system is to be operated in this mode, a small entrance hatch will allow the removal and replacement of filters on the ND filter wheel. This will allow filters which simulate the TM (or other satellite) bands to be inserted as desired. Figure 1b is a diagram of the system.

The opto-mechanical layout is shown in Figs. 2, 3 and 4 and represent top, side and front views of the instrument. We want to keep the instrument as simple as possible and yet still be able to operate in either automatic or manual mode. We also want to make it as lightweight as possible in order to make it portable. As seen in Figs. 2 and 4, the spectral and neutral density filter wheels are laterally spaced very close together. This configuration minimizes the lateral dimension while still allowing access to each wheel for manual operation. Two stepper motors will drive them. The lens and baffle assembly is a self-contained unit directly behind the spectral filter wheel. The waveplate and polarizer should be moved together when making measurements, so their movements have been synchronized using a rotating cam. This cam will enable the waveplate to be in position for half the measurements and to be replaced by a dummy waveplate for the other half. The polarizer rotates using a gear and pulley system and as it rotates the waveplate slides in and out. The two aperture wheels are also tied together physically and thus require only one stepper motor as does the polarizer/waveplate system. The polarizer is mounted in a bearing and is

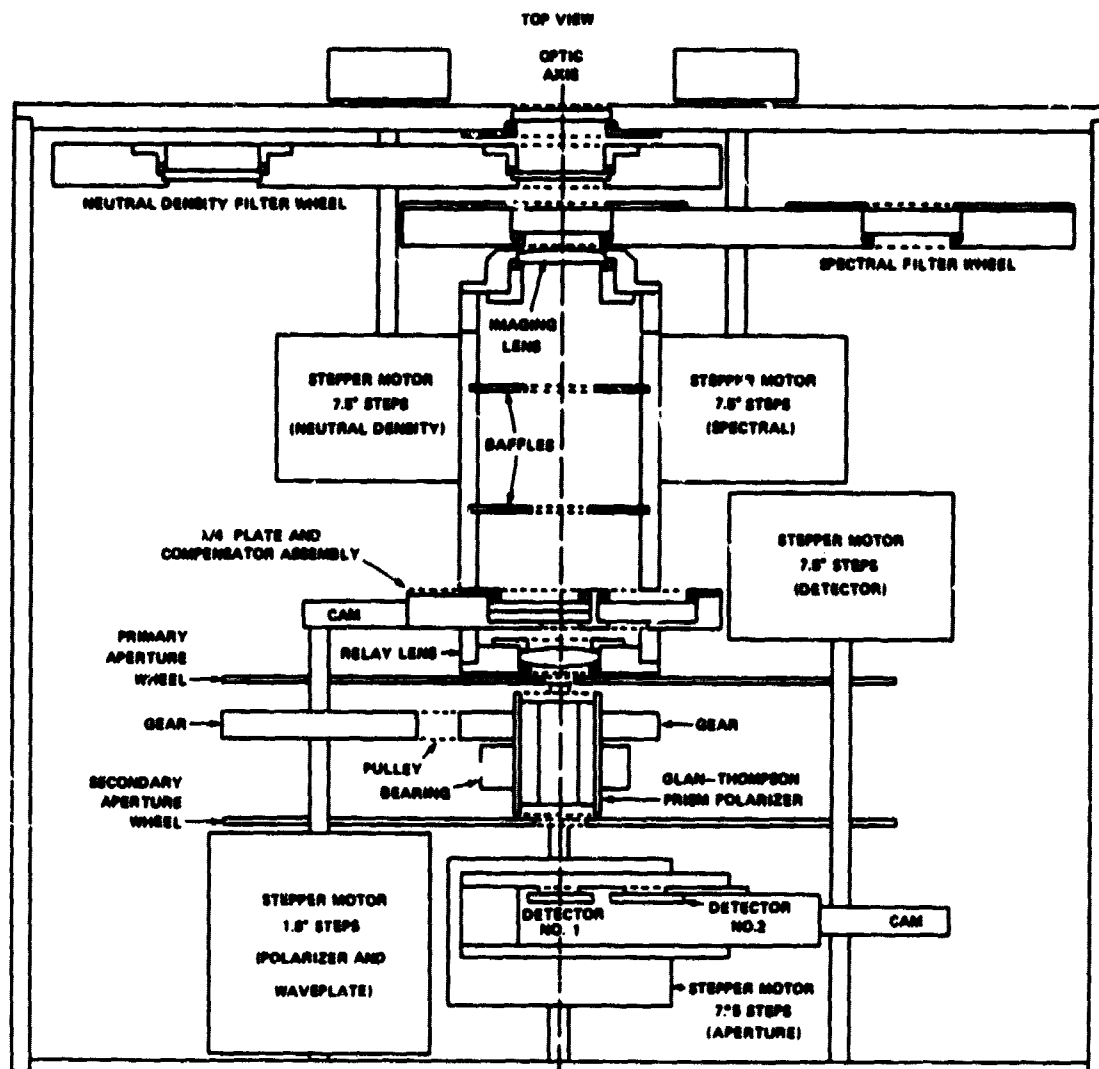


Fig. 2. Top view of opto-mechanical instrument layout.

ORIGINAL PAGE IS
OF POOR QUALITY

SIDE VIEW

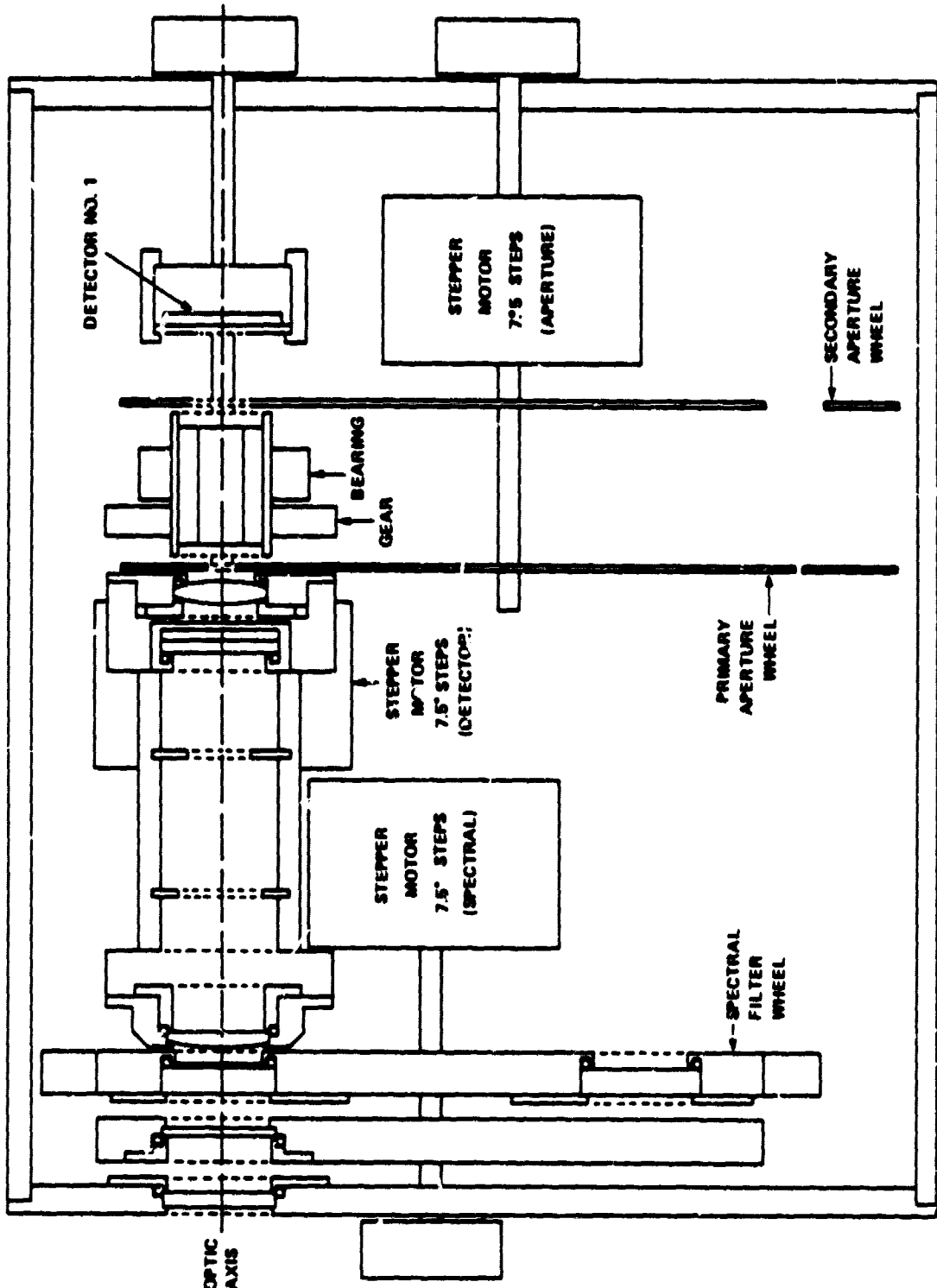


Fig. 3. Side view of opto-mechanical instrument layout.

ORIGINAL FILM IS
OF POOR QUALITY

14

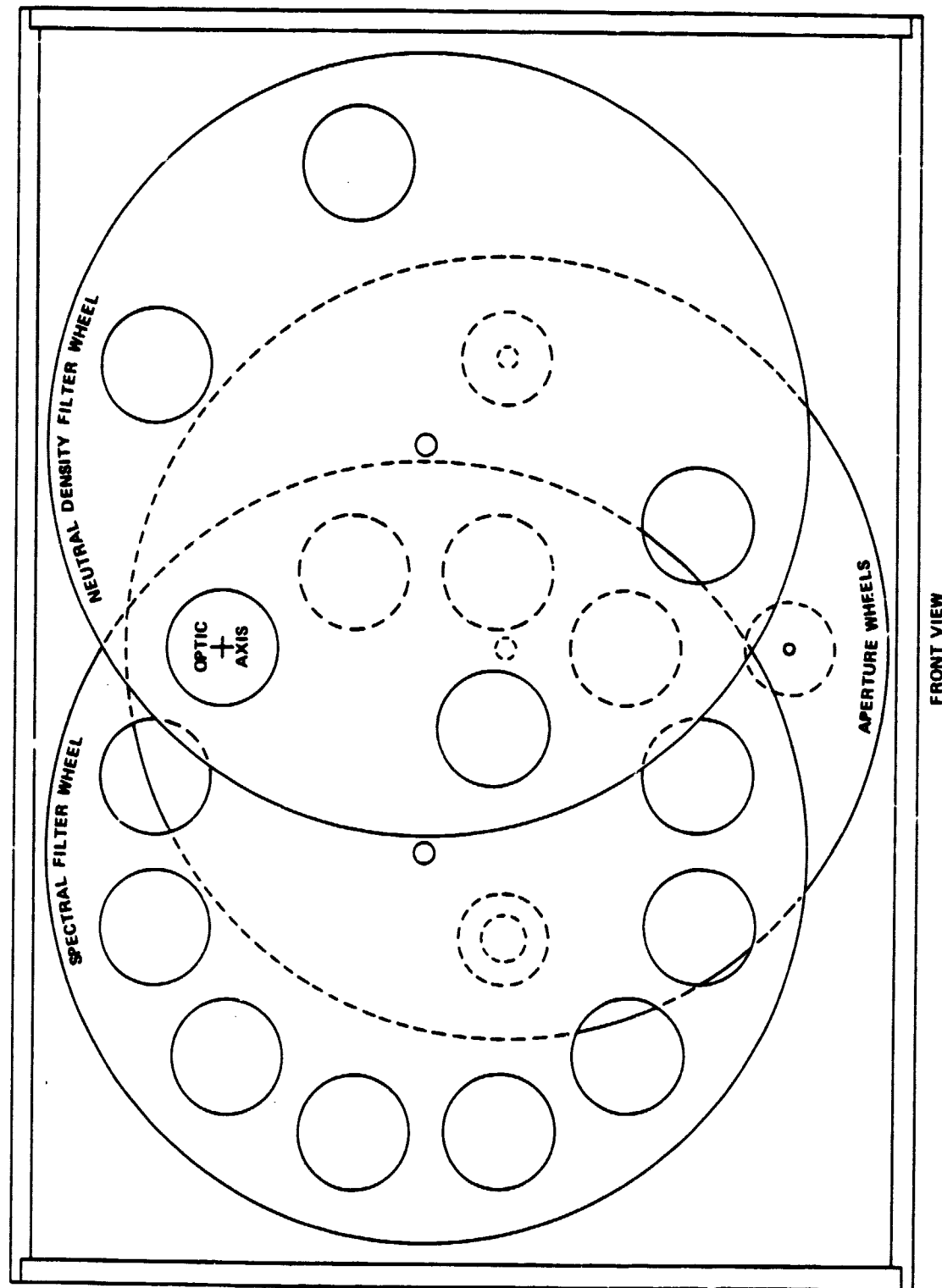


Fig. 4. Front view of opto-mechanical instrument layout.

very carefully positioned between the two aperture wheels. It has also been decided to mount the two detectors so they can be slid in and out of view as desired. This requires a fifth stepper motor which is located as shown in Figs. 2 and 3. All the drives can also be driven manually and the entire package fits in a box 8"x10"x11" (20x25x27.5cm). The front face is 8"x11" (20x27.5cm) and will block approximately 1.5 percent of the sky when used in the ground-looking configuration from a 2 meter height above the ground.

Two identical instruments will be built for taking simultaneous measurements of the ground, sun and sky, and to provide some redundancy.

It is planned to operate these instruments using a microcomputer with data storage occurring on a magnetic disk. A permanent mount will be built for one instrument for alt-azimuth tracking the sun and sky while the other instrument will be mounted on a cart for ground measurements. Final configurations will be discussed in the next report.

REFERENCES

1. G. E. Shaw, J. A. Reagan, B. M. Herman, "Investigations of atmospheric extinction using direct solar radiation measurements with a multiple wavelength radiometer," *J. Appl. Meteor.* 12, 347 (1973).
2. G. E. Shaw, "Solar spectral radiance and atmospheric transmission at Manna Loa Observatory," *Appl. Opt.* 21, 2006 (1982).

3. Use of these products does not constitute an endorsement, etc.
4. W. P. Elkins, "A spectral polarimeter for the analysis of atmospheric aerosols," Masters thesis, University of Arizona, 1983.